

Recurrent generation of maximally entangled single particle states via quantum walks on cyclic graphs

Dinesh Kumar Panda^{1,2,*} and Colin Benjamin^{1,2,†}

¹*School of Physical Sciences, National Institute of Science Education and Research Bhubaneswar, Jatni 752050, India*

²*Homi Bhabha National Institute, Training School Complex, Anushaktinagar, Mumbai 400094, India*

Maximally entangled single particle states (MESPS) are opening new possibilities in quantum technologies as they have the potential to encode more information and are robust to decoherence compared to their non-local two-particle counterparts. Herein, using discrete-time quantum walks on k -cycles where $k \in \{3, 4, 5, 8\}$ and by using either a single coin or effective-single coin or two coins in various deterministic sequences, we generate MESPS for recurring time steps. These sequences beget ordered quantum walks and yield MESPS with periods 4, 6, 9, 12, and 15. For the first time, we reveal single coins such as Hadamard, which can generate periodic MESPS (with periods 4 and 12) on 4 and 8-cycles. This scheme is resource-saving with possibly the most straightforward experimental realization since the same coin is applied at each time step.

Introduction.— Hybrid or single particle entanglement (SPE) refers to the entanglement between different degrees of freedom such as spatial mode, polarization, and orbital angular momentum belonging to the same particle[1]. This local entanglement enables encoding more information at the single particle level, is more robust against decoherence, and has simpler experimental implementation than its non-local bipartite counterpart[1–3]. SPE has significant applications in photonic quantum information processing and analysis of states of photons, elementary particles and quantum liquids[1]. Quantum joining, a physical process that allows the transfer of intra-particle entanglement between photons into a single output photon’s hybrid entanglement and its inverse, has been reported, and it has applications in quantum networking[4]. Photonic SPE states are potentially advantageous in optical quantum networks because they enable a more flexible network with every photon transmitted via a suitable channel [5]. SPE has also been used in experimental tests of non-contextual hidden variable theories[1].

After their introduction in [6], quantum walks(QWs), apart from their use in quantum computation, have been used in designing efficient quantum algorithms[7–9] as well as in simulating dynamics of complex physical[10] and biological systems[11]. QWs can also be directly implemented in laboratories without requiring a quantum computer[12]. Experimentally, quantum walks have already been realized with photons[3, 13, 14], trapped ions[15, 16], superconducting qubits[17, 18], neutral atoms[19, 20], NMR quantum information processors[21] and ultra-cold Rubidium-87 atoms[22]. The quantum walker (or particle) is represented by a wave function and obeys the quantum superposition principle, and this makes QWs superior compared to their classical counterparts [6]. A discrete-time quantum walk (DTQW) evolves by repeatedly applying two quantum opera-

tors: coin and shift. DTQW dynamics also works as a sophisticated tool in engineering arbitrary quantum states[23, 24]. DTQWs allow one to explore multi-path quantum interference [20, 25], and numerous non-trivial topological[26] and geometrical phenomena[27]. A quantum walk can be described on a 1D or 2D lattice and analogously on a cyclic graph with k sites (k -cycle). For some detailed studies on quantum walks on k -cycles, see Refs.[28–30]. Ref.[30] reports on the experimental implementation of QW on cyclic graphs with photons using linear optical elements. A recent work [31] shows that it is possible to design an ordered or periodic QW (i.e., the walker returns to a particular position or site periodically after a finite number of time steps) by combining two chaotic or non-periodic quantum walks on 3– or 4–cycle via Parrondo strategy[32]. Intriguingly, the emergence of order from chaos and its inverse in QWs has applications in quantum cryptography (secure encryption-decryption protocols[31]), in designing new quantum algorithms and in developing theory of quantum chaos control[33].

Several manuscripts recently reported that DTQWs on 1D lines could be efficient tools to generate entangled single-particle states(SPS) or SPE, see Refs.[2, 3, 34–39]. Refs.[3, 35] report on experimental realizations of SPE generation. One recent manuscript [34] shows that by incorporating Parrondo sequences of coin operators in DTQWs on 1D line, one can obtain phase-independent SPE and, in one case, maximal SPE independent of the initial state parameters for time steps of 3 and 5.

There has been no attempt to generate maximally entangled SPS (MESPS) or, for that matter SPE in cyclic graphs. Also, seeing the versatility of DTQWs and the preminent applicability of SPE, exploring different methods to generate highly or maximally entangled SPS via DTQWs is an important task, as it would contribute to extending the horizons of quantum technologies [1]. Our aim in this work is to study the propensity of DTQWs on cyclic graphs in generating MESPS either using a single coin or, an effective-single coin (i.e., coin operator followed by Identity operator at successive time steps) or two coins in a deterministic evolution operator

* dineshkumar.quantum@gmail.com

† colin.nano@gmail.com

sequence and, their relation to ordered QW dynamics.

QW model.— A DTQW on a k -cycle (Fig. 1), similar to that on a 1D lattice, is defined on a tensor product of position (H_P) and coin (H_C) Hilbert spaces, i.e., $H = H_P \otimes H_C$. H_C is associated with the coin (or qubit) and has the computational basis $\{|0_c\rangle, |1_c\rangle\}$, whereas H_P , is the k -dimensional position space for the walker with computational basis $\{|x_p\rangle : x_p \in \{0, 1, 2, \dots, k-1\}\}$. If the walker is initially localized at the site $|0_p\rangle$ in a general superposition of the coin states, it is represented by,

$$|\psi_i\rangle = |\psi(t=0)\rangle = \cos(\theta/2) |0_p 0_c\rangle + e^{i\phi} \sin(\theta/2) |0_p 1_c\rangle, \quad (1)$$

with $\theta \in [0, \pi]$ and $\phi \in [0, 2\pi]$. The unitary coin operator, in general, is,

$$\hat{C}_2(\rho, \gamma, \eta) = \begin{pmatrix} \sqrt{\rho} & \sqrt{1-\rho}e^{i\gamma} \\ \sqrt{1-\rho}e^{i\eta} & -\sqrt{\rho}e^{i(\gamma+\eta)} \end{pmatrix}, \quad (2)$$

where $0 \leq \rho \leq 1$ and $0 \leq \gamma, \eta \leq \pi$.

The walker moves to the left by one site for coin state $|0_c\rangle$ and to the right by one site for coin state $|1_c\rangle$. For the walker on the k -cycle, we use the shift operator $\hat{S} = \sum_{q=0}^1 \sum_{j=0}^{k-1} |(j+2q-1 \pmod{k})_p\rangle \langle j_p| \otimes |q_c\rangle \langle q_c|$. The full evolution now can be expressed as,

$$U_k(t) = \hat{S} \cdot [I_k \otimes \hat{C}_2(\rho(t), \gamma(t), \eta(t))], \quad (3)$$

where I_k is a $k \times k$ identity matrix. The time-evolution of the system (quantum walker) after time steps t is then,

$$\begin{aligned} |\psi(t)\rangle &= U_k(t) |\psi(t-1)\rangle = U_k(t)U_k(t-1)\dots U_k(1) |\psi(0)\rangle \\ &= \sum_{j=0}^{k-1} [\alpha_1(j, t) |j_p, 0_c\rangle + \alpha_2(j, t) |j_p, 1_c\rangle], \end{aligned} \quad (4)$$

where, $\alpha_1(j, t)$ and $\alpha_2(j, t)$ are amplitudes for the states $|j_p, 0_c\rangle$ and $|j_p, 1_c\rangle$ respectively. Further, the QW is said to be ordered or periodic if the walker reverts to its initial state after a time step, say $t = N$, irrespective of the choice of the initial quantum state. For an ordered QW with period N , we may write,

$$|\psi(N)\rangle = U_k(N)U_k(N-1)\dots U_k(1) |\psi_i\rangle = |\psi_i\rangle. \quad (5)$$

For simplicity, if we apply a particular coin operator in the above QW evolution, i.e., $U_k(t) = U_k(t-1) = \dots U_k(1) = U_k(\text{say})$, then Eq. (5) is equivalent to, $U_k^N |\psi_i\rangle = \sum_{i=1}^{2k} a_i \lambda_i^N |\lambda_i\rangle$, wherein the arbitrary $|\psi_i\rangle$ is expressed in terms of the eigenvalues $\{\lambda_i\}$ and eigenvectors $\{|\lambda_i\rangle\}$ of U_k , i.e., $|\psi_i\rangle = \sum_{i=1}^{2k} a_i |\lambda_i\rangle$. Clearly, from Eq. (5), the condition of periodicity for the quantum walk follows as: $U_k^N = I_{2k}$ or $\lambda_i^N = 1, \forall i \in \{1, 2, \dots, 2k\}$. Any unitary evolution operator which satisfies this condition gives a periodic probability distribution for the walker's position, and such an operator is said to yield

ordered QW. Otherwise, the QW is said to be chaotic. Furthermore, to simplify the problem of finding the eigenvalues of U_k and hence the periodicity of the QW on a k -cycle, the 2×2 block circulant matrix U_k is block diagonalized by using commensurate Fourier matrix tool as was done in Ref.[28]. Then the block diagonalized form of U_k is given by $F U_k F^\dagger = \text{diag}[U_{k,0}, U_{k,1}, \dots, U_{k,k-1}]$, wherein $F = F^k \otimes F^2$ with F^M being an $M \times M$ commensurate Fourier matrix i.e., $F^M = (F_{m,n}^M) = \frac{1}{\sqrt{M}} (e^{2\pi i \frac{mn}{M}})$ where $m, n = 0, 1, \dots, M-1$. The periodicity condition is satisfied if the eigenvalues $\lambda_{k,l}^\pm$ of each block $U_{k,l}$ take the form of de Moivre numbers ($e^{2\pi i \frac{m_r}{n_r}}$) where each (m_r, n_r) pair is coprime [28, 31] or, equivalently if, $\lambda_{k,l}^{U_k} = \frac{\lambda_{k,l}^+ + \lambda_{k,l}^-}{2} = e^{2\pi i \frac{m_r}{n_r}}$, and $N = \text{LCM}(\{n_r\})$, with $r \in \{1, 2, \dots, 2k\}$. In Refs.[28, 29], examples of parameter values for U_k that satisfy the periodicity condition have been given (i.e., to obtain ordered QWs). We discuss a unique analytical approach for obtaining values of such parameters viz. $\{\rho, \gamma, \eta\}$ yielding ordered QWs with deterministic (including Parrondo type) evolution operator sequences in *Results*.

Measuring Entanglement.— The initial quantum state in Eq. (1) is pure and evolves unitarily via DTQW. We use Schmidt norm(S) to quantify the entanglement between the coin and position degrees of freedom of the time-evolved quantum state $|\psi(t)\rangle$. It is relatively more convenient to calculate for QWs [2, 40–42]. Let ρ_ψ be density operator for $|\psi(t)\rangle$ i.e., $\rho_\psi = |\psi(t)\rangle \langle \psi(t)|$ and reduced density operator (ρ_c) for the coin space can be defined by, $\rho_c \equiv \text{Tr}_p(\rho_\psi)$, where the partial trace Tr_p is taken over the position degrees of freedom. We write the eigenvalues of the reduced density matrix ρ_c as, $E_\pm = \frac{1}{2} \pm |\vec{n}|$, where, $\vec{n} = \left(\text{Re}(\sum_j \alpha_1(j, t) \alpha_2^*(j, t)), \text{Im}(\sum_j \alpha_1(j, t) \alpha_2^*(j, t)), \frac{1}{2} \sum_j (|\alpha_1(j, t)|^2 - |\alpha_2(j, t)|^2) \right)$. Finally, the Schmidt norm is given by, $S = \sqrt{E_-} + \sqrt{E_+}$, and for the present system with $\min(\dim H_P, \dim H_C) = 2$, the Schmidt norm for the case of a MESPS is $\sqrt{2}$ [34]. To check whether our results are correct, we also calculate entanglement entropy (E) which is the von-Neumann entropy for the reduced density matrix ρ_c of coin state. E is defined as $E(\rho_c) = -\text{Tr}(\rho_c \log_2 \rho_c)$ with 0 and 1 for separable and maximally entangled states (or, MESPS) respectively, and can be calculated via, $E = -(E_-) \log_2(E_-) - (E_+) \log_2(E_+)$. Indeed we see identical results for MESPS via both the entanglement measures, see Supplementary Material Sec. A.

Results.— We consider the following coin operators, see Eq. (2), Hadamard coin $\hat{H} = \hat{C}_2(\rho = \frac{1}{2}, \gamma = 0, \eta = 0)$, Grover or flip coin $\hat{X} = \hat{C}_2(\rho = 0, \gamma = 0, \eta = 0)$, and Identity coin $\hat{I} = \hat{C}_2(\rho = 1, \gamma, \eta \ni \gamma + \eta = \pi)$. We execute several numerical experiments with these coin operators and, also, by forming multiple deterministic coin evolution sequences[34] such as $A_k A_k A_k$, $A_k B_k A_k A_k B_k A_k \dots$, $A_k B_k A_k B_k \dots$, $A_k B_k B_k A_k B_k B_k \dots$, $A_k A_k B_k A_k A_k B_k \dots$

etc., where, $A_k = U_k(\rho_1, \gamma_1, \eta_1) = \hat{S} \cdot [I_k \otimes \hat{C}_2(\rho_1, \gamma_1, \eta_1)]$ and $B_k = U_k(\rho_2, \gamma_2, \eta_2) = \hat{S} \cdot [I_k \otimes \hat{C}_2(\rho_2, \gamma_2, \eta_2)]$. If $\hat{C}_2 = \hat{H}$, then evolution operator is denoted as $H_k = U_k(\frac{1}{2}, 0, 0) = \hat{S} \cdot [I_k \otimes \hat{H}]$. Similarly, if $\hat{C}_2 = \hat{X}$, we have evolution operator $X_k = U_k(0, 0, 0) = \hat{S} \cdot [I_k \otimes \hat{X}]$, and if $\hat{C}_2 = \hat{I}$, then evolution operator $I_k = U_k(1, 0, \pi) = \hat{S} \cdot [I_k \otimes \hat{I}]$. The primary idea behind such experiments was to reveal evolution operator sequences involving either two coins such as $H_k H_k X_k \dots$, $H_k X_k H_k X_k \dots$ etc. or, effective-single coin (i.e., I_k with either H_k or X_k) such as $I_k H_k I_k \dots$, $H_k I_k I_k \dots$, $H_k I_k H_k I_k \dots$ etc., or, notably a single coin such as $H_k H_k H_k \dots$ wherein the same coin \hat{H} is applied at every time step of the QW, which yield MESPS along with rendering ordered QWs. We first discuss single-coin evolution sequences, then effective single-coin evolution sequences and finally, two-coin evolution sequences to generate MESPS via DTQWs on the cyclic graphs.

Note that from an experimental point of view, a QW for a single coin evolution sequence like $H_k H_k H_k \dots$ is the simplest in terms of experimental setup as it just uses the same coin \hat{H} at each time step [30]. In other words, the same setup will be sufficient for its realization in small and significant time steps. Further, effective-single coin evolution sequences like $I_k H_k I_k \dots$ or $H_k I_k I_k \dots$ consists of just a single coin (here \hat{H}) and their implementation are indeed resource-saving because no device is required for Identity coin operation in the experimental realization of the associated QW [3].

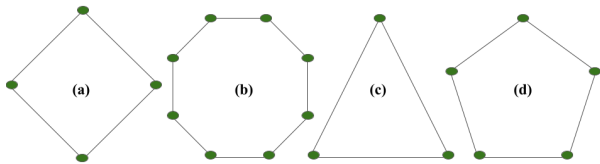


FIG. 1: Even: 4-cycle (a) and 8-cycle (b) graphs; Odd: 3-cycle (c) and 5-cycle (d) graphs, with sites in green dots.

MESPS on 4- and 8-cycle graphs. — We now consider even i.e., 4-cycle ($k = 4$) and 8-cycle ($k = 8$) graphs, as shown in Fig. 1. Fig. 2(red) shows the Schmidt norm values as functions of time steps(t), generated by the single coin evolution sequence $H_4 H_4 H_4 \dots$ on the 4-cycle, wherein each data point is an average of the Schmidt norm (S_{av}) and the average is taken over θ with fixed $\phi = \frac{\pi}{2}$ and is evaluated as, $S_{av} = \langle \frac{S}{\sqrt{2}} \rangle = \frac{1}{\pi} \int_0^\pi d\theta \frac{S}{\sqrt{2}}$. Clearly, for maximal SPE or MESPS, $S_{av} = 1$. We observe that the single coin evolution sequence $H_4 H_4 H_4 \dots$ yields periodic MESPS at time steps $t = 1, 5, 9, \dots$ with period 4. Also, for 8-cycle case, single coin evolution sequence $H_8 H_8 H_8 \dots$ yields periodic MESPS at $t = 1, 13, 25, \dots$ with period 12, shown in Fig. 2. The periodic behaviour of $H_k H_k H_k \dots$ in generating MESPS is supported by its ordered QW dynamics on both $k = 4$ and $k = 8$ cycle graphs, see Supplementary Material

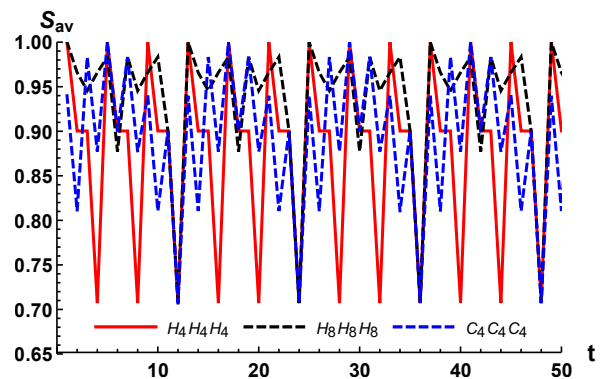


FIG. 2: Average Schmidt norm S_{av} versus time steps(t) with single coin evolution sequences $H_4 H_4 H_4 \dots$, $C_4 C_4 C_4 \dots$ for 4-cycle and $H_8 H_8 H_8 \dots$ for 8-cycle.

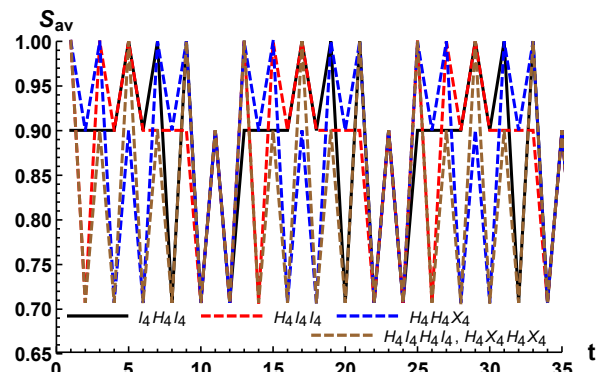


FIG. 3: S_{av} versus time steps(t) with sequences: $I_4 H_4 I_4 \dots$, $H_4 I_4 I_4 \dots$, $H_4 I_4 H_4 I_4 \dots$, $H_4 H_4 X_4 \dots$, $H_4 X_4 H_4 X_4 \dots$, for 4-cycle.

Sec. A.

We now discuss effective-single coin evolution sequences $I_4 H_4 I_4 \dots$, $H_4 I_4 I_4 \dots$ and $H_4 I_4 H_4 I_4 \dots$ designed from the coin set $\{\hat{H}, \hat{I}\}$ with the 4-cycle. From Fig. 3 we see that the S_{av} values generated via the sequence $I_4 H_4 I_4 \dots$ follow a periodic trend. This observation is well supported by the periodic probability distribution $P(x = 0)$ for the walker position at $|0_p\rangle$, in other words, the sequence $I_4 H_4 I_4 \dots$ not only generates MESPS at $t = 5, 7, 9, 17, \dots$ with period 12 but also an ordered quantum walk (see Supplementary Material Sec. A). Analytically one can also prove this by exploiting the periodicity condition, beginning with the eigenvalues of the $U_{4,1}$ -block of the evolution operator (U_4)³, see Eq. 3, $\lambda_{4,1}^{U_4 U_4 U_4} = \frac{1}{2} i \sqrt{\rho} e^{\frac{3}{2} i(\gamma+\eta)} (e^{-\frac{1}{2} i(\gamma+\eta)} + e^{\frac{1}{2} i(\gamma+\eta)}) (-3 + 2\rho + (e^{-i(\eta+\gamma)} + e^{i(\eta+\gamma)})\rho)$. Similarly, the $U_{4,1}$ -block's eigenvalues for the sequence $I_4 H_4 I_4$ give, $\lambda_{4,1}^{I_4 H_4 I_4} = \frac{i}{\sqrt{2}}$. Equating $\lambda_{4,1}^{U_4 U_4 U_4}$ with $\lambda_{4,1}^{I_4 H_4 I_4}$ for $\delta = (\gamma + \eta) = 0$, we get $\rho = \frac{2 + \sqrt{3}}{4}$, which is an exact match with ρ obtained in Ref.[28] for a periodic QW with periodicity $N = 24$. With this analytical description for

$I_4H_4I_4\dots$ sequence giving an ordered QW, we observe that single coin evolution sequence $C_4C_4C_4\dots$ (i.e., coin $\hat{C}_2(\rho = \frac{2+\sqrt{3}}{4}, \gamma = 0, \eta = 0)$ applied at each time step) generates MESPS with period 12 at $t = 5, 17, 29, \dots$, see Fig. 2. This periodicity is supported by the ordered QW dynamics of the $\hat{C}_2(\frac{2+\sqrt{3}}{4}, 0, 0)$ coin, see Supplemental Material Sec. A, again with $N = 24$. Moreover, effective single coin evolution sequences $H_4I_4I_4\dots$ and $H_4I_4H_4I_4\dots$ yield periodic MESPS with periods 12 and 4 at time steps $t = 1, 3, 5, 13, \dots$ and $t = 1, 5, 9, \dots$ respectively, see Fig. 3.

We also observe that two-coin evolution sequence $H_4H_4X_4\dots$ gives recurring MESPS with period 6 at time steps $t = 1, 3, 7, 9, 13, \dots$ (proof of this periodicity is in Supplemental Material Sec. A), whereas the sequence $H_4X_4H_4X_4\dots$ gives recurring periodic MESPS with period 4 at $t = 1, 5, 9, \dots$, for 4-cycle, see Fig. 3.

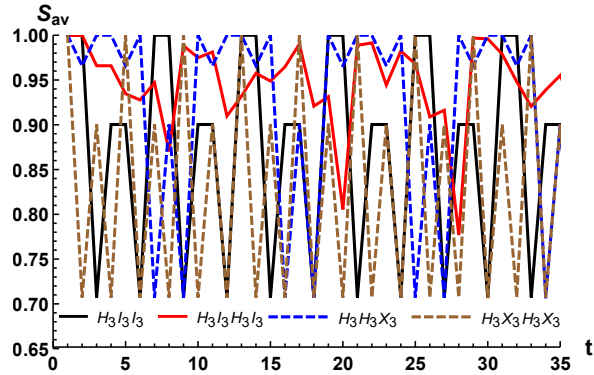


FIG. 4: S_{av} versus time steps(t) with sequences: $H_3I_3I_3\dots$, $H_3I_3H_3I_3\dots$, $H_3H_3X_3\dots$, $H_3X_3H_3X_3\dots$, for 3-cycle.

MESPS on 3- and 5-cycle graphs.— Moving now to odd cycles, a 3-cycle ($k = 3$) and a 5-cycle ($k = 5$), see Fig. 1. Unfortunately, for both 3 and 5-cycles, we do not see periodic MESPS with single coin evolution sequences $H_kH_kH_k\dots$, $X_kX_kX_k\dots$, $I_kI_kI_k\dots$, however, $H_kH_kH_k\dots$ generates MESPS at time step $t = 1$ but renders chaotic QWs. In case of 3-cycle, the effective single coin evolution sequence $H_3I_3I_3\dots$ yields periodic MESPS with period 6 at $t = 1, 2, 7, 8, \dots$, but the sequence $I_3H_3I_3\dots$ renders ordered QWs without MESPS, whereas $H_3I_3H_3I_3\dots$ renders chaotic QW with MESPS at $t = 1, 2$ (see Fig. 4). Further, in the case of 5-cycle, we see that the evolution sequences $I_5H_5I_5\dots$, $H_5I_5I_5\dots$, and $H_5I_5H_5I_5\dots$ do not yield periodic MESPS. But these sequences generate MESPS at $t = 3, 4$, $t = 1, 2, 3, 4$ and, $t = 1, 2, 3$ respectively, as shown in Fig. 5 (also see Supplemental Material Sec. A).

From Fig. 4, we observe that the two-coin evolution sequences $H_3H_3X_3\dots$ and $H_3X_3H_3X_3\dots$ generate recurring as well as periodic MESPS respectively at $t = 1, 3, 4, 6, 10, \dots$ (with period 9) and $t = 1, 5, 9, \dots$ (with period 4) via the DTQW on the 3-cycle (for proof of this periodicity, see Supplementary Material Sec. A). Moreover, we see MESPS in the 5-cycle case via sequence

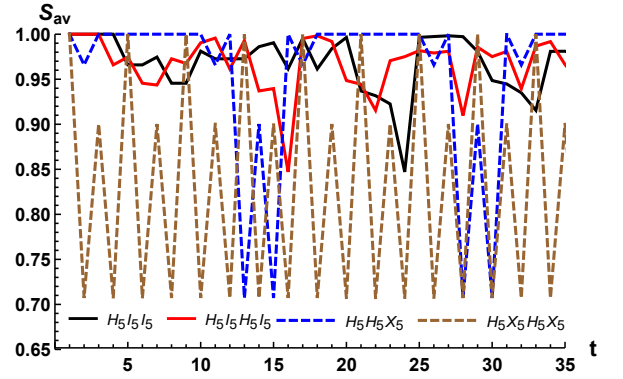


FIG. 5: S_{av} versus time steps(t) with sequences: $H_5I_5I_5\dots$, $H_5I_5H_5I_5\dots$, $H_5H_5X_5\dots$, $H_5X_5H_5X_5\dots$, for 5-cycle.

$H_5H_5X_5\dots$ at $t = 1, 3, 4, 5, 6, 7, 8, 9, 10, 12, 16, \dots$ with period 15, while via $H_5X_5H_5X_5\dots$ sequence at $t = 1, 5, 9, \dots$ with period 4, see Fig. 5.

The above results on MESPS generation are juxtaposed in Supplementary Material Sec. B, where one can compare our proposed evolution sequences on these cyclic graphs. We see that employing $H_3H_3X_3\dots$, $H_3I_3I_3\dots$, and $H_3X_3H_3X_3\dots$ on a 3-cycle one can obtain MESPS at all time steps up to 10, whereas on a 4-cycle their analogues give MESPS at all odd time steps $t \leq 10$, see Figs. 3 and 4. As these sequences also beget periodic QWs, thus, one obtains MESPS at larger time steps ($t > 10$) as well. Moreover, it is interesting to observe that with just sequences $H_5H_5X_5\dots$ and $H_5I_5I_5\dots$, one can generate MESPS for all time steps $t \leq 10$ and also at larger t , on a 5-cycle, see Fig. 5. In fact, only $H_5H_5X_5\dots$ by itself yields MESPS at time steps $t = 1, 3, 4, 5, 6, 7, 8, 9, 10, 12, 16, \dots$ with period 15.

It is for the first time we report the single coin evolution sequences $H_4H_4H_4\dots$ and $C_4C_4C_4\dots$ which individually yields periodic MESPS on a 4-cycle graph with periods 4 and 12 respectively, see Fig. 2. Apart from that, we showed that $H_8H_8H_8\dots$ generates periodic MESPS at $t = 1, 13, 25, \dots$ (with period 12) on a 8-cycle. The generation of periodic MESPS with just a single coin such as \hat{H} or $\hat{C}_2(\frac{2+\sqrt{3}}{4}, 0, 0)$ via DTQWs, is a milestone in resource-saving SPE generation schemes and is also the simplest scheme in the field of controlled entanglement generation till date, as it would require the same experimental setting for its realization for both small and large time steps [3, 30].

Conclusions.— This letter provides a novel scheme to generate maximally entangled single particle states via DTQWs on both odd (3,5)- and even (4,8)-cycle graphs, with just a single coin and with both resource-saving effective-single coin and two-coin deterministic evolution sequences. It is shown that with a 4-cycle, the single-coin evolution sequences: $H_4H_4H_4\dots$, $C_4C_4C_4\dots$; the effective single coin evolution sequences: $I_4H_4I_4$, $H_4I_4I_4\dots$, $H_4I_4H_4I_4\dots$; and finally, the two-coin evolution

sequences: $H_4H_4X_4\dots$, $H_4X_4H_4X_4\dots$ individually yield periodic recurring MESPS with periods 4, 12, 12, 12, 4, 6 and 4 respectively. Moreover, these sequences render the associated quantum walks periodic, and an analytical proof of this result has been established. Finally, we show MESPS generation via DTQWs on 3- and 5-cycles, too, wherein we see that apart from begetting ordered QWs, the sequences $H_3I_3I_3\dots$, $H_3H_3X_3\dots$, and $H_3X_3H_3X_3\dots$, generate recurring MESPS with periods 6, 9, and 4 respectively, for the 3-cycle case. In the 5-cycle case, the sequences $H_5H_5X_5\dots$ and $H_5X_5H_5X_5\dots$ yield MESPS with periods 15 and 4 respectively. In Supplementary Material Sec. B, we summarize the proposed coin evolution sequences to generate MESPS at time steps up to 10 and beyond with the cyclic graphs.

One can experimentally implement our proposed scheme using linear optical elements such as half-wave plates (HWPs), quarter wave plates (QWPs) and polarizing beam splitters (PBSs), along with a fast switching electro-optical modulator (EOM), wherein the photon's polarization degree of freedom encodes the coin state with the position state is encoded into different time bins of the photon [30, 37]. Evaluating the Schmidt norm requires post-processing measurements like average polarizations of the photon by proper arrangement of an HWP and QWP[37, 43].

A comparison of our work with other relevant works

(DTQWs on 1D line) is shown in Supplementary Material Sec. C. Apart from opening a unique avenue for MESPS generation, our letter significantly outperforms other schemes in terms of model simplicity and resource-saving architecture and periodically yields MESPS at both small and large time steps.

Our findings naturally raise new intriguing research questions: What is the interplay between disorder and entanglement (both hybrid and non-local) generation for 1D or higher dimensional walkers? Can this scheme be adapted to improve existing cryptography protocols [31, 44]? Investigations into these directions may lead to significant results which foster new local or non-local entanglement generation schemes.

Our presented work will significantly contribute towards state-of-art controlled (maximal) entanglement generation protocols, which is a fundamental resource in quantum computing, teleportation and cryptography and hence, a prerequisite to constructing reliable devices for quantum information processing tasks.

Acknowledgement.— Colin Benjamin would like to thank Science and Engineering Research Board (SERB) for funding under the Core Research grant "Josephson junctions with strained Dirac materials and their application in quantum information processing," Grant No. CRG/2019/006258.

-
- [1] S. Azzini, S. Mazzucchi, V. Moretti, D. Pastorello, and L. Pavesi, Single-Particle Entanglement, *Advanced Quantum Technologies* 3, 2000014 (2020).
 - [2] A. Gratsea, M. Lewenstein, and A. Dauphin, Generation of hybrid maximally entangled states in a one-dimensional quantum walk, *Quantum Science and Technology* 5, 025002 (2020).
 - [3] Xiao-Xu Fang, Kui An, Bai-Tao Zhang, Barry C. Sanders, He Lu, Maximal entanglement between a quantum walker and her quantum coin for the third step and beyond regardless of the initial state (2022), arXiv:2209.01727 [quant-ph]
 - [4] C. Vitelli, N. Spagnolo, F. Sciarrino, E. Santamato, and L. Marrucci, Joining the quantum state of two photons into one, *Research in Optical Sciences, OSA Technical Digest (Optical Society of America, 2014)*, paper QW3B.2.(2014).
 - [5] G. Zhu, L. Xiao, B. Huo, and P. Xue, Photonic discrete-time quantum walks, *Chinese Optics Letters* 18, 052701 (2020).
 - [6] Y. Aharonov, L. Davidovich, and N. Zagury, Quantum random walks, *Phys. Rev. A* 48, 1687 (1993).
 - [7] R. Portugal, *Quantum Walks and Search Algorithms* (Springer, 2019).
 - [8] A. Ambainis, Quantum search algorithms, *SIGACT News* 35, 22 (2004)
 - [9] V. Kendon, A random walk approach to quantum algorithms, *Philos. Trans. R. Soc., A* 364, 3407 (2006).
 - [10] Kunkun Wang, Xingze Qiu, Lei Xiao, Xiang Zhan, Zhihao Bian, Wei Yi, and Peng Xue, Simulating Dynamic Quantum Phase Transitions in Photonic Quantum Walks, *Phys. Rev. Lett.* 122, 020501 (2019)
 - [11] Masoud Mohseni, Patrick Rebentrost, Seth Lloyd, and Alán Aspuru-Guzik, Environment-assisted quantum walks in photosynthetic energy transfer, *J. Chem. Phys.* 129, 174106 (2008).
 - [12] Karuna Kadian, Sunita Garhwal, Ajay Kumar, Quantum walk and its application domains: A systematic review, *Computer Science Review*, 41 (2021) 100419.
 - [13] F. Cardano, et al., quantum walks and wave packet dynamics on a lattice with twisted photons, *Science Advances* 1, 15516 (2015).
 - [14] A. Schreiber, K. N. Cassemiro, V. Potocek, A. Gabris, P. J. Mosley, E. Andersson, I. Jex, and C. Silberhorn, Photons walking the line: A quantum walk with adjustable coin operations, *Phys. Rev. Lett.* 104, 050502 (2010).
 - [15] H. Schmitz, R. Matjeschk, C. Schneider, J. Glueckert, M. Enderlein, T. Huber, and T. Schaetz, Quantum walk of a trapped ion in phase space, *Phys. Rev. Lett.* 103, 090504 (2009).
 - [16] F. Zahringer, et al., realization of a quantum walk with one and two trapped ions, *Physical Review Letters* 104, 100503 (2010).
 - [17] J.-Q. Zhou, L. Cai, Q.-P. Su, and C.-P. Yang, Protocol of a quantum walk in circuit QED, *Phys. Rev. A* 100, 012343 (2019).
 - [18] E. Flurin, V. Ramasesh, S. Hacoheh-Gourgy, L. Martin, N. Yao, and I. Siddiqi, Observing topological invariants using quantum walks in superconducting circuits, *Physical Review X* 7, 031023 (2017).

- [19] M. Karski, L. Forster, J.-M. Choi, A. Steffen, W. Alt, D. Meschede, and A. Widera, Quantum walk in position space with single optically trapped atoms, *Science* 325, 174–177 (2009).
- [20] C. Robens, S. Brakhane, D. Meschede, and A. Alberti, Quantum walks with neutral atoms: Quantum interference effects of one and two particles, *Laser Spectroscopy*, 1-15 (2016).
- [21] C. A. Ryan, M. Laforest, J. C. Boileau, and R. Laflamme, Experimental implementation of a discrete-time quantum random walk on an NMR quantum-information processor, *Phys. Rev. A* 72, 062317 (2005).
- [22] K. Manouchehri and J. Wang, Quantum random walk with Rb atoms, *Journal of Physics: Conference Series* 185, 012026 (2009).
- [23] L. Innocenti, et al., Quantum State Engineering Using One-dimensional Discrete-time Quantum Walks, *Frontiers in Optics/Laser Science*, OSA Technical Digest (Optical Society of America, 2018), paper JW3A.72.
- [24] T. Giordani, et al., Experimental Engineering of Arbitrary Qudit States with Discrete-Time Quantum Walks, *Phys. Rev. Lett.* 122, 020503 (2019).
- [25] A. Crespi, R. Osellame, R. Ramponi et al., Integrated multimode interferometers with arbitrary designs for photonic boson sampling. *Nature Photon.* 7, 545–549 (2013).
- [26] Vikash Mittal, Aswathy Raj, Sanjib Dey and Sandeep K. Goyal, Persistence of topological phases in non-Hermitian quantum walks, *Sci Rep* 11, 10262 (2021).
- [27] G. Puentes, Topology and holonomy in discrete-time quantum walks, *Crystals* 7, 122 (2017).
- [28] Phillip R. Dukes, Quantum state revivals in quantum walks on cycles, *Results in Physics* 4, 189-197 (2014)
- [29] Ben Tregenna, Will Flanagan, Rik Maile and Viv Kendon, *New J. Phys.* 5, 83 (2003).
- [30] Zhi-Hao Bian, Jian Li, Xiang Zhan, Jason Twamley, and Peng Xue, Experimental implementation of a quantum walk on a circle with single photons, *Phys. Rev. A* 95, 052338 (2017)
- [31] Abhisek Panda and Colin Benjamin, Order from chaos in quantum walks on cyclic graphs, *Phys. Rev. A* 104, 012204 (2021)
- [32] G. P. Harmer and D. Abbott, Losing strategies can win by Parrondo’s paradox, *Nature* 402, 864 (1999).
- [33] B. Whaley and G. Milburn, Focus on coherent control of complex quantum systems, *New J. Phys.* 17, 100202 (2015).
- [34] Dinesh Kumar Panda, B. Varun Govind, Colin Benjamin, Generating highly entangled states via discrete-time quantum walks with Parrondo sequences, *Physica A: Statistical Mechanics and its Applications* 608, 128256 (2022).
- [35] S. Li, H. Yan, Y. He, and H. Wang, Experimentally feasible generation protocol for polarized hybrid entanglement, *Phys. Rev. A* 98, 022334 (2018).
- [36] C. M. Chandrashekar, Disorder induced localization and enhancement of entanglement in one and two-dimensional quantum walks (2012), arXiv:1212.5984[quant-ph].
- [37] R. Vieira, E. P. M. Amorim, and G. Rigolin, Dynamically disordered quantum walk as a maximal entanglement generator, *Phys. Rev. Lett.* 111, 180503 (2013).
- [38] R. Vieira, E. P. M. Amorim, and G. Rigolin, Entangling power of disordered quantum walks, *Phys. Rev. A* 89, 042307 (2014).
- [39] A. Gratsea, F. Metz, and T. Busch, Universal and optimal coin sequences for high entanglement generation in 1D discrete time quantum walks, *Journal of Physics A: Mathematical and Theoretical* 53, 445306 (2020).
- [40] M. B. Plenio, Logarithmic negativity: A full entanglement monotone that is not convex, *Phys. Rev. Lett.* 95, 090503 (2005)
- [41] R. Hildebrand, Concurrence revisited, *Journal of Mathematical Physics* 48, 102108 (2007).
- [42] D. Janzing, Entropy of entanglement, *Compendium of Quantum Physics*, 205–209 (2009).
- [43] A. Peres, *Quantum Theory: Concepts and Methods* (Kluwer Academic, New York, 2002).
- [44] C. Vlachou et al., Quantum walk public-key cryptographic system, *Int. J. Quantum Inf.* 13, 1550050 (2015).
- [45] Rong Zhang et al., Maximal coin-walker entanglement in a ballistic quantum walk, *Phys. Rev. A* 105, 042216 (2022)

SUPPLEMENTARY MATERIAL

Here in Sec. A, we provide some more details of our results, which includes the generation of maximally entangled single-particle states (MESPS) and non-maximal single particle entanglement (SPE) via single-coin, effective-single coin and two-coin evolution sequences. The proof for periodicity in QW dynamics and the occurrence of periodic MESPS via two coin evolution sequences is also provided. We tabulated our proposed evolution sequences yielding MESPS for comparison in Sec. B. Finally, we compare our work with other relevant works in Sec. C.

A. MESPS and periodicity of QWs

4-cycle

The analytical and numerical studies on MESPS generation via DTQWs on cyclic graphs, dealt in the main text, for the 4-cycle case with the single coin evolution sequence $H_4H_4H_4\dots$ and the effective-single (i.e., a single coin from the experimentalist's point of view) coin evolution sequences: $I_4H_4I_4\dots$, $H_4I_4I_4\dots$, $H_4I_4H_4I_4\dots$, yield recurring MESPS with periods 4, 12, 12, and 4 respectively. We also generate periodic MESPS with two-coin evolution sequences $H_4H_4X_4\dots$, and $H_4X_4H_4X_4\dots$ with periods 6 and 4, respectively.

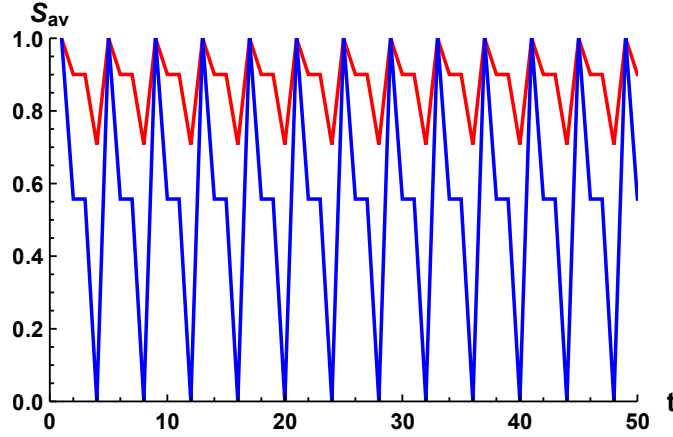


FIG. 6: Average Schmidt norm S_{av} (red) and average entanglement entropy E_{av} (blue) versus time steps (t) with single-coin evolution sequence $H_4H_4H_4\dots$, for 4-cycle.

Fig. 6 shows the Schmidt norm and entanglement entropy values as functions of time steps(t), generated by the single coin evolution sequence $H_4H_4H_4\dots$ on the 4-cycle, wherein each data point is an average of the Schmidt norm (S_{av}) or the entanglement entropy (E_{av}) and the average is taken over θ with fixed $\phi = \frac{\pi}{2}$, and is evaluated as, $S_{av} = \langle \frac{S}{\sqrt{2}} \rangle = \frac{1}{\pi} \int_0^\pi d\theta \frac{S}{\sqrt{2}}$, or, $E_{av} = \langle E \rangle = \frac{1}{\pi} \int_0^\pi E d\theta$. Since both give identical results for MESPS, i.e., $S_{av} = E_{av} = 1$, we only calculate S_{av} in the letter. One can also observe that the sequence $H_4H_4H_4\dots$ generates MESPS at time steps $t = 1, 5, 9, \dots$ with period 4 (via any of the entanglement measures). Its ordered QW dynamics support this periodicity, as shown in Fig. 7, which shows periodic probability distribution $P(x = 0)$ for the walker position at $|0_p\rangle$ with sequence $H_4H_4H_4\dots$ for 4-cycle, along with those via sequences $H_8H_8H_8\dots$ for 8-cycle and $C_4C_4C_4\dots$ for 4-cycle.

In the main text, we observe that the two-coin evolution sequence $H_4H_4X_4\dots$ gives recurring MESPS periodic in time for the 4-cycle. This periodicity is supported by ordered QW dynamics of $H_4H_4X_4$ which is shown in Fig. 8. Its analytical proof, following the steps involved in the periodicity condition, begins with the eigenvalues of the $U_{4,1}$ block of the evolution operator $(U_4)^3$,

$$\lambda_{4,1}^{U_4U_4U_4} = \frac{1}{2} i\sqrt{\rho} e^{\frac{3}{2}i(\gamma+\eta)} (e^{-\frac{1}{2}i(\gamma+\eta)} + e^{\frac{1}{2}i(\gamma+\eta)}) (-3 + 2\rho + (e^{-i(\eta+\gamma)} + e^{i(\eta+\gamma)})\rho), \quad (6)$$

then for sequence $H_4H_4X_4$, we have,

$$\lambda_{4,1}^{H_4H_4X_4} = -i, \quad (7)$$

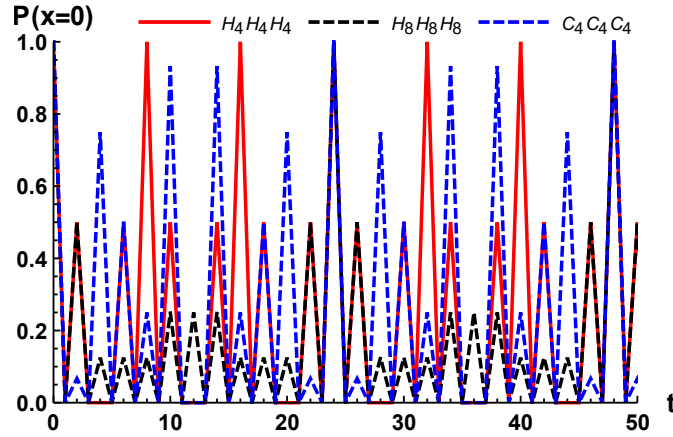


FIG. 7: Probability $P(x = 0)$ of finding the walker at position $|0_p\rangle$ as function of time steps(t) with the single coin evolution sequences $H_4H_4H_4\dots$, $C_4C_4C_4\dots$ for 4-cycle, and $H_8H_8H_8\dots$ for 8-cycle.

from which we get for $\delta = (\gamma + \eta) = 0$, $\rho = \frac{1}{4}$, which is an exact match to the value noted in Ref.[28] to generate an ordered QW on a 4-cycle (with periodicity $N = 12$). Thus, $H_4H_4X_4\dots$ renders periodic QW as shown in Fig. 8.

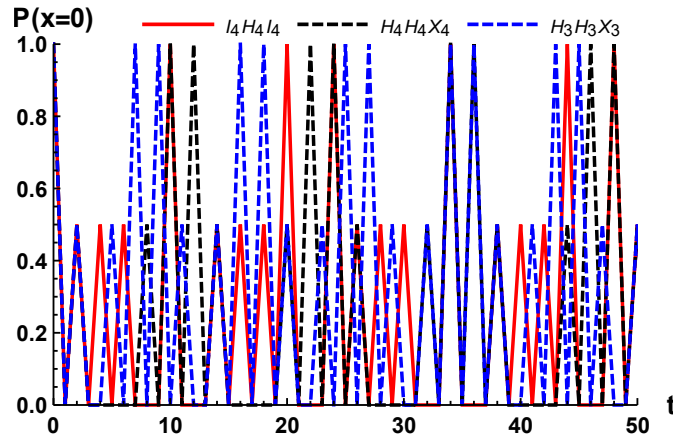


FIG. 8: Probability $P(x = 0)$ of finding the walker at position $|0_p\rangle$ as function of time steps(t) with the evolution sequences $I_4H_4I_4\dots$, $H_4H_4X_4\dots$ for 4-cycle, and $H_3H_3X_3\dots$ for 3-cycle.

The evolution sequences above yield better results as compared to the single coin evolution sequences $X_4X_4X_4\dots$ and $I_4I_4I_4$ since these do not generate MESPS. This is clearly seen in Fig. 9, where the average Schmidt norm (S_{av}) values from the sequence $H_4H_4H_4\dots$ are compared with those from $X_4X_4X_4\dots$ and $I_4I_4I_4\dots$ sequences, for 4-cycle. Though, $X_4X_4X_4\dots$ and $I_4I_4I_4$ beget ordered QWs, they do not yield MESPS.

3-cycle and 5-cycle

Results for DTQW on 3- and 5-cycle graphs yield effective single-coin evolution sequences and two-coin evolution sequences that result in MESPS, but no single-coin evolution sequence was found for the odd (3,5) cycle graphs. However, sequence $H_kH_kH_k\dots$ gives MESPS only at time step $t = 1$ for $k = 3$ and $k = 5$ -cycle graphs, see Figs. 10-11. This is unlike the sequence $H_4H_4H_4\dots$ for the 4-cycle case, which gives MESPS at $t = 1, 5, 9\dots$ with period 4, as discussed in the main text.

Further, the effective single coin evolution sequence $I_3H_3I_3\dots$ renders ordered QWs without MESPS for 3-cycle, whereas the evolution sequences $I_5H_5I_5\dots$ renders chaotic QWs but with MESPS at $t = 3, 4$ for 5-cycle, as shown in Fig. 12. On the other hand, $I_4H_4I_4\dots$ begets ordered QWs as well as periodic MESPS at $t = 5, 7, 9, 17, \dots$ with period

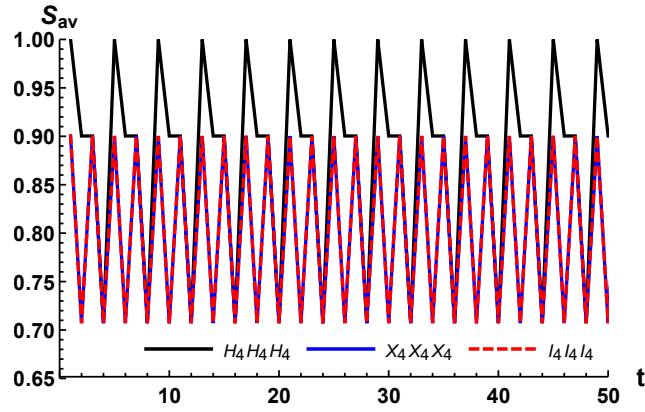


FIG. 9: S_{av} as function of time steps(t) with single coin evolution sequences: $H_4 H_4 H_4 \dots$, $X_4 X_4 X_4 \dots$, $I_4 I_4 I_4 \dots$, for 4-cycle graph.

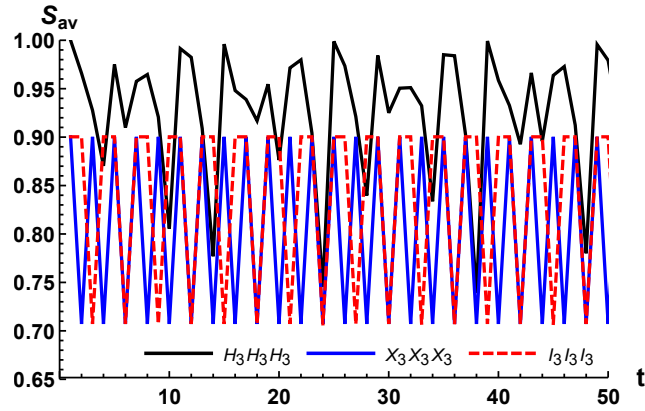


FIG. 10: S_{av} as function of time steps(t) with single coin evolution sequences: $H_3 H_3 H_3 \dots$, $X_3 X_3 X_3 \dots$, $I_3 I_3 I_3 \dots$, for 3-cycle graph.

12 (also see, Fig. 8).

In the main text, we also observe that the two-coin evolution sequences $H_k H_k X_k \dots$ and $H_k X_k H_k X_k \dots$ yield recurring and periodic MESPS for both 3- and 5-cycle graphs. A similar analytical proof for the periodic behaviour of $H_3 H_3 X_3 \dots$ on the 3-cycle can also be shown. Firstly, we get for the eigenvalues of the $U_{3,1}$ block of the evolution operator $(U_3)^3$,

$$\lambda_{3,1}^{U_3 U_3 U_3} = \frac{1}{4} \sqrt{\rho} (3(1 + i\sqrt{3})e^{i(\eta+\gamma)}(\rho - 1) + 3i(i + \sqrt{3})e^{2i(\eta+\gamma)}(\rho - 1) + 2\rho - 2e^{3i(\eta+\gamma)}\rho), \quad (8)$$

and then for the sequence $H_3 H_3 X_3$, we have,

$$\lambda_{3,1}^{H_3 H_3 X_3} = -\frac{i\sqrt{3}}{2}, \quad (9)$$

from which $\rho = 0.550901$, 0.15597 , which match the values noted in Ref.[28] to generate an ordered QW on a 3-cycle (with periodicity $N = 18$). Thus, $H_3 H_3 X_3 \dots$ renders periodic QW dynamics as shown in Fig. 8.

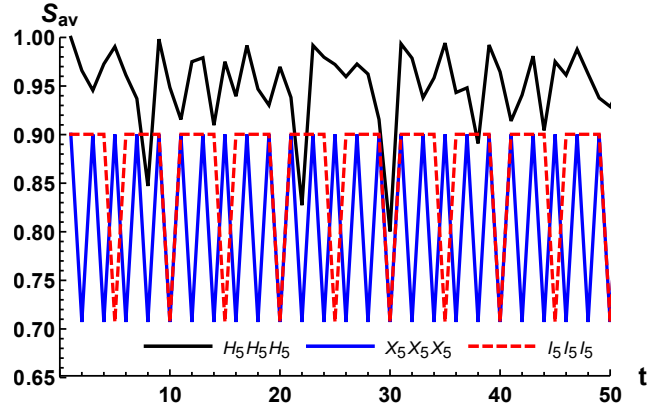


FIG. 11: S_{av} as function of time steps(t) with single coin evolution sequences: $H_5 H_5 H_5 \dots$, $X_5 X_5 X_5 \dots$, $I_5 I_5 I_5 \dots$, for 5-cycle graph.

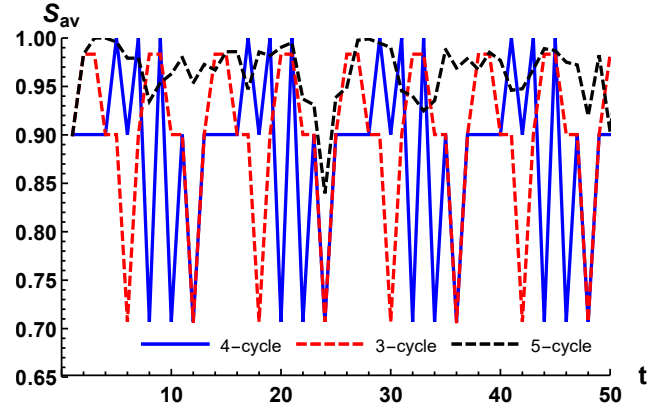


FIG. 12: S_{av} for effective single coin evolution sequence $I_k H_k I_k \dots$ up to 50 time steps(t), for $k \in \{3, 4, 5\}$ i.e., 3-, 4- and 5-cycle graphs.

B. Our proposed evolution sequences

We summarize our proposed coin evolution sequences to generate recurring and periodic MESPS at time steps up to 10 and beyond with the cyclic graphs in Table I

TABLE I: Evolution sequences to generate MESPS via DTQW up to 10-time steps and beyond periodically

DTQW on 4-cycle and 8-cycle	DTQW on 3-cycle and 5-cycle
Single coin evolution sequences: $H_4 H_4 H_4 \dots$ at $t = 1, 5, 9, \dots$ ($P = 4$) $C_4 C_4 C_4 \dots$ at $t = 5, 17, 29, \dots$ ($P = 12$) $H_8 H_8 H_8 \dots$ at $t = 1, 13, 25, \dots$ ($P = 12$)	Single coin evolution sequences: $H_3 H_3 H_3 \dots$ at $t = 1$ (Chaotic) $H_5 H_5 H_5 \dots$ at $t = 1$ (Chaotic)
Effective single coin evolution sequences: $I_4 H_4 I_4 \dots$ at $t = 5, 7, 9, 17, \dots$ ($P = 12$) $H_4 I_4 I_4 \dots$ at $t = 1, 3, 5, 13, \dots$ ($P = 12$) $H_4 I_4 H_4 I_4 \dots$ at $t = 1, 5, 9, \dots$ ($P = 4$)	Effective single coin evolution sequences: $I_3 H_3 I_3 \dots$ (No maximal SPE, periodic) $H_3 I_3 I_3 \dots$ at $t = 1, 2, 7, 8, \dots$ ($P = 6$) $H_3 I_3 H_3 I_3 \dots$ at $t = 1, 2$ (Chaotic) $I_5 H_5 I_5 \dots$ at $t = 3, 4$ (Chaotic) $H_5 I_5 I_5 \dots$ at $t = 1, 2, 3, 4$ (Chaotic) $H_5 I_5 H_5 I_5 \dots$ at $t = 1, 2, 3$ (Chaotic)
Two coin evolution sequences: $H_4 H_4 X_4 \dots$ at $t = 1, 3, 7, 9, 13, \dots$ ($P = 6$) $H_4 X_4 H_4 X_4 \dots$ at $t = 1, 5, 9, \dots$ ($P = 4$)	Two coin evolution sequences: $H_3 H_3 X_3 \dots$ at $t = 1, 3, 4, 6, 10, \dots$ ($P = 9$) $H_3 X_3 H_3 X_3 \dots$ at $t = 1, 5, 9, \dots$ ($P = 4$) $H_5 H_5 X_5 \dots$ at $t = 1, 3 - 10, 12, 16, \dots$ ($P = 15$) $H_5 X_5 H_5 X_5 \dots$ at $t = 1, 5, 9, \dots$ ($P = 4$)
$t \rightarrow$ time steps, $P \rightarrow$ Period at which the sequence yields maximal SPE	

C. A comparison of our scheme and results with other relevant works

We compare our scheme and results with other relevant works[2, 3, 34, 39, 45] in Table II. We first compare the type of coin (evolution) sequences and the number of coin operators used. Here, we use single coin and effective single coin evolution sequences(i.e., 'single' from an experimental point of view) and deterministic evolution sequences of two coin operators. Ref. [34] uses deterministic Parrondo type two-coin evolution sequences and has considered four different coin operators. In Refs. [2, 39] coin sequences based on optimization and a deterministic sequence, namely- universal entangler[39] are proposed. Ref. [3] uses a rigorous optimization scheme to obtain efficient coin sequences with quantum process fidelity as the cost function. Ref.[45] deals with inhomogeneous QW, where they use position-dependent coin operations. Experimental realization is straightforward with less number of coin operators being involved and with a small number of sites. Given this, our proposed sequences (single, effective-single and two coin evolution sequences) are as good as the entangling sequences of [2, 3, 34, 39, 45] and are much simpler to work with. Moreover, our work involves only 3, 4or5–sites for the QW evolution, which is also resource-saving.

TABLE II: Comparison of the present work with other relevant works

Properties/Model→	This Paper (4-cycle with single coin: \hat{H} or $\hat{C}_2(\frac{2+\sqrt{3}}{4}, 0, 0)$)	This Paper (3,4,5-cycles with effective-single coin or two-coin evolution sequences)	With Parrondo sequences Refs. [34]	With Optimization Ref. [3]	Analysis with inhomogeneous-QW Ref. [45]	With Optimization Ref. [2]	With Optimization Ref. [39]
No. of coin operators used	One coin \hat{H} or $\hat{C}_2(\rho = \frac{2+\sqrt{3}}{4}, \gamma = 0, \eta = 0)$	Effective-single coin or, 2 coins	Two-coin sequences	Hadamard and Identity coins	2 coins inhomogeneously	Full set of possible coin operators	2 coins
Procedure	Simple, single coin QW on cyclic graph	Simple, QW with deterministic evolution sequences on cyclic graph	QW on 1D line with Parrondo sequences	Optimization with QW on 1D line	Inhomogeneous QW on 1D line	Basin hopping algorithm, QW on 1D line	RL technique, QW on 1D line
Maximally entangled states	At time steps(t), $t = 1, 5, 9, \dots$ (with $H_4 H_4 H_4 \dots$, $P = 4$); moreover at, $t = 5, 17, 29, \dots$ (with $C_4 C_4 C_4 \dots$, $P = 12$). Both single-coin evolution sequences $H_4 H_4 H_4 \dots$ and $C_4 C_4 C_4 \dots$ individually yield periodic MESPS. ($P \rightarrow$ Period at which the sequence yields MESPS.)	At time steps(t), $t = 1, 3, 4, 6, 10, \dots$ ($H_3 H_3 X_3 \dots$, $P = 9$); $t = 1, 2, 7, 8, \dots$ ($H_3 I_3 I_3 \dots$, $P = 6$); $t = 1, 5, 9, \dots$ ($H_k X_k H_k X_k \dots$, $k = 3, 4, 5$, $P = 4$); moreover, at $t = 1, 3, 10, 12, 16, \dots$ ($H_5 H_5 X_5 \dots$, $P = 15$); $t = 1, 2, 3, 4$ ($H_5 I_5 I_5 \dots$, Chaotic); $t = 5, 7, 9, 17, \dots$ ($I_4 H_4 I_4 \dots$, $P = 12$), etc. So MESPS $\forall t \leq 10$ and larger t . And periodic emergence of MESPS.	At $t = 3, 5$ and at asymptotic t	At $t = 3$ and beyond	At any odd t and asymptotically in even t	Almost at $t = 10$ and beyond	Not achieved

Additionally, the focus on a small number of time steps in Ref. [2] shows maximal entanglement can be achieved in 10-time steps and beyond. Ref.[3] generates maximal entanglement via the optimization problem for any time step beyond the second, whereas Ref.[45] shows maximal entanglement can be generated for any odd time steps, and in the asymptotic limit for even steps. The method proposed in Ref. [34] gives MESPS in 3 and 5 time steps independent of the initial states. Our scheme shows the generation of MESPS at all time steps(t) up to 10 as well as at a larger t with periodic occurrence (see, Table I).